

TOWARD THE FOURTH INDUSTRIAL REVOLUTION: TESTING THE CAPABILITY OF MACHINE LEARNING IN PREDICTING NORMAL GRAVITY

Bernard KUMI-BOATENG, Faculty of Mineral Resources Technology, Department of Geomatic Engineering, University of Mines and Technology, Tarkwa, Ghana, kumi@umat.edu.gh

Yao Yevenyo ZIGGAH, Faculty of Mineral Resources Technology, Department of Geomatic Engineering, University of Mines and Technology, Tarkwa, Ghana, yyziggah@umat.edu.gh

Abstract: *As the world enters the fourth industrial revolution of Artificial Intelligence (AI), Internet of Things (IoT), robotics, virtual and augmented reality, researchers like geodesist have been challenged with the task to apply and ascertain the capabilities of such technologies in solving real life problems. Machine learning which a subset of AI is increasingly being applied as alternative predictive tool to solve geospatial problems. In this study, the normal gravity is considered. The objective of the presented work is to test the capabilities of machine learning approaches (strengths and weaknesses) in evaluating (predicting) normal gravity. Looking at the current fourth industrial revolution where machine learning is at its centre stage, the main motivation of this study is to seek answers to the following questions: can machine learning be used to create a normal gravity prediction model?; and can the machine learning model predict normal gravity values with sufficient accuracy? In line with these questions, the study applied the supervised learning approach to develop Backpropagation Neural Network (BPNN), Radial Basis Function Neural Network (RBFNN), Group Method of Data Handling (GMDH), Support Vector Machine (SVM), Least Squares Support Vector Machine (LSSVM) and Multivariate Adaptive Regression Splines (MARS) models. Statistical analysis revealed good prediction accuracy for all the proposed models. In comparison, the RBFNN achieved the best RMSE, NRMSE, MAPE, VAF and PI values of 2.93E-05 mGal, 5.97E-10%, 2.20E-09%, 99% and 1.9, respectively.*

Keywords: *Machine Learning, Normal Gravity Field, Somigliana-Pizzetti formula, Reference Ellipsoid*

1. Introduction

The introduction of terrestrial, airborne and satellite gravimetric surveys in geosciences has revolutionised the understanding of earth geometry and its subsurface structure. The gathered gravity data from such surveys has been widely used for several geoscience applications. For example, in geodetic sciences, the observed gravity data has enabled geodesist to rigorously determine different height systems with their respective gravimetric corrections (Yilmaz, 2008; Kingdon, 2012). Besides, the geoid can now be determined to a centimetre level of accuracy (Abbak and Ustun, 2015). Looking at the Gravity Recovery and Climate Experiment (GRACE) data, hydro geodesists can estimate the total water storage in all the major basins of lakes and rivers across the globe (Wang et al., 2015; Hasan and Jin, 2016). The GRACE data has also been applied to flood and drought studies by considering its effect on food security (Awange and Kiema, 2013; Cao et al., 2015;

Anyah, 2018; Forootan, 2019). In geophysics and geology, gravity data is used to study the earth crust by identifying and providing enough information to understand the various lithologies and layers of the earth interior (Rybakov, 2000; Leaman and Webster, 2002; Sedlak, 2007; González et al., 2010). It is widely known that to achieve the enumerated gravimetric survey applications, rigorous analysis and interpretation of the observed gravity data is required to convert such measurements into gravity anomalies. To carry out the conversion, knowledge of the corresponding normal (theoretical) gravity of the earth for the observed gravity values must be known.

The concept of the normal gravity was introduced as the second approximation of the earth due to the equipotential ellipsoid of revolution (Li and Götze, 2001). The essence is to reduce the magnitude of gravity variations locally, regionally and globally by referring the actual gravity field to a radial field (Vanicek and Krakiwsky, 1986; Jacoby and Smilde, 2009). In this way, the oblateness of the earth could be absorbed by correcting for the latitude in gravity measurements.

Historically, one of the first attempts to define the normal gravity cited in Moritz (1980) was given by Paolo Pizzetti in 1894 which was later worked on by Carlo Somigliana in 1929 and adopted in 1930 by the International Union of Geodesy and Geophysics (IUGG) at a conference in Stockholm. However, over the years, several approximate and closed form mathematical solutions have been proposed to define the normal gravity with respect to different geodetic reference systems. Notable approximate solutions include the Helmert 1901 gravity formula and International Gravity Formulas (IGF) 1930, 1967, 1980 and 1984 which correspond to Helmert 1906, International 1924, Geodetic Reference System (GRS) 67, GRS 80 and World Geodetic System (WGS) 84 as their respective reference ellipsoids (Hans-Jürgen, 2011). In literature, the closed-form solutions for calculating the normal gravity at any point on, above or below the ellipsoid surface can be found in Heiskanen and Moritz (1967); Lakshmanan, (1991); Li and Götze, (1996).

Studies into assessing the efficiency of the approximate and closed-form solutions in different jurisdictions have been extensively investigated by several researchers (Osazuwa, 1993; Li and Götze, 2001; Vadja and Pánisová, 2005; Isioye, 2010; Okiwelu et al., 2010). Comparative studies of these methods have revealed sufficient information on their computational strengths and weaknesses in different countries. However, evidence from literature suggests that the Somigliana-Pizzetti formula (Ardalan and Grafarend, 2001) is the most rigorous and can successfully be applied across the globe to compute the normal gravity with minimum degree of uncertainties (Li and Götze, 2001).

As the world enters the fourth industrial revolution of Artificial Intelligence (AI), Internet of Things (IoT), robotics, virtual and augmented reality, researchers like geodesists have been challenged with the task to apply and ascertain the capabilities of such technologies in solving real life problems. Machine learning which a subset of AI is increasingly being used as alternative predictive tool in geodesy. The objective of the presented work is to test the capabilities of machine learning approaches (strengths and weaknesses) in evaluating (predicting) normal gravity. Taking cognizant of the fact that machine learning is at centre stage of the current fourth industrial revolution, the authors were motivated to seek answers to the following questions: can supervised machine learning be used to create a normal gravity

prediction model?; and can the machine learning model predict normal gravity values with sufficient accuracy?

This study therefore used the supervised machine learning approach to model and predict normal gravity. The supervised learning approach has been widely and successfully applied to solve different geodetic problems such as tide modelling (Salim et al., 2015; Wang and Yuan, 2018), coordinate transformation (Gullu and Narin, 2019; Ziggah et al., 2019 and references therein), gravity anomalies estimation (Tierra and De Freitas, 2005; Kaftan et al., 2011; Kenfack et al., 2011), digital terrain model height prediction (Okwuashi and Ndehedehe, 2015), crustal deformation and landslide modelling (Huang et al., 2016 and references therein), Global Navigation Satellite System (GNSS) error modelling (Razin and Voosoghi, 2017; Dabove and Manzano, 2017), earth orientation parameter modelling (Liao et al. 2012; Lei et al. 2015) and prediction of observed gravity field (Turgut, 2016). The reported results are favourable and suggest the need for one to further explore the practicality of the supervised learning approach in the area of normal gravity prediction. Moreover, the use of machine learning as a modelling technique offers appropriate adaptability to data patterns and flexibility in the model building process.

Reviews of literature have shown that, until now, no studies have applied machine learning techniques to predict normal gravity. Considering the valuable contributions of the normal gravity to geodetic sciences and its allied disciplines, this study sought to apply, develop and select the optimum machine learning model for predicting normal gravity in Ghana. To accomplish that, a supervised machine learning algorithm was used to map a mathematical function from the input variables to the output variable. The objective is to correctly define the mapping function so that when new input data is introduced, the machine learning system can accurately predict the outputs. Therefore, to satisfy the supervised machine learning condition, the computed normal gravity values from the Somigliana-Pizetti formula was used as the output variable and latitude, longitude and elevation of the observed gravity positions were used as the input variables in the machine learning methods. This study therefore applied six different machine learning techniques. They include Backpropagation Neural Network (BPNN), Radial Basis Function Neural Network (RBFNN), Group Method of Data Handling (GMDH), Support Vector Machine (SVM), Least Squares Support Vector Machine (LSSVM) and Multivariate Adaptive Regression Splines (MARS). These methods were selected because they have been the most widely and successfully used in geodetic sciences (Okwuashi and Ndehedehe, 2015; Wang and Yuan, 2018; Ziggah et al., 2019 and references therein). In addition, it is a challenge to identify the best performing machine learning approach because of variation in the geographic extent of coordinates from country to country. Therefore, experimenting on different approaches is known to be an efficient way of finding out the best machine learning technique (Nguyen, 2019) for predicting normal gravity in the study area (Ghana). In order for the authors to make objective assessments of the prediction models, statistical performance indicators of Mean Absolute Percentage Error (MAPE), Normalised Root Mean Square Error (NRMSE), Root Mean Square Error (RMSE), Variance Accounted For (VAF) and Performance Index (PI) were employed.

The rest of the paper is presented as follows: Section 2 provides the study area information and data used. Section 3 provides overview of the machine learning techniques applied. Section 4 provides information on the various performance metrics used to assess

model quality. Section 5 presents the various acceptable trained models for normal gravity field prediction. Sections 6 discusses the results while conclusions are given in Section 7.

2. Materials and Methods

2.1 Study Area and Data Used

The study area is located between latitude $4^{\circ} 30' N$ and $11^{\circ} N$, and from longitude $3^{\circ} W$ to $1^{\circ} E$ (Mugnier, 2000) which covers the whole of Ghana. Two separate historical data sets consisting of latitudes, longitudes, elevations and observed terrestrial gravity were acquired and put together from Bureau Gravimétrique International (BGI) and Ziwu (2011). The data captured in Ziwu (2011) was provided by then Geological Survey Department now Ghana Geological Survey Authority. For the case of BGI, a request was made for the data to be used strictly for research purposes by the authors. All together, the study applied a total of 424 data sets of observed gravity locations that is spread across the entire country. The spatial distribution of the observed gravity positions and basic statistics of the entire data set is presented in Table 1 and Figure 1.

Table 1. Statistical Description of Input and Output Variables for the Entire Data used to Develop the Normal Gravity Prediction Models (Total Observation = 424)

Variables	Symbol	Unit	Minimum	Maximum	Mean	Median	Standard Deviation
Latitude	φ	($^{\circ}$)	4.883	10.955	7.739	7.554	1.730
Longitude	λ	($^{\circ}$)	-3.107	1.215	-1.345	-1.648	1.090
Elevation	H	M	2.740	491.000	190.195	194.730	98.795
Normal Gravity	γ	mGal	978070.093	978219.180	978130.822	978121.9	43.282

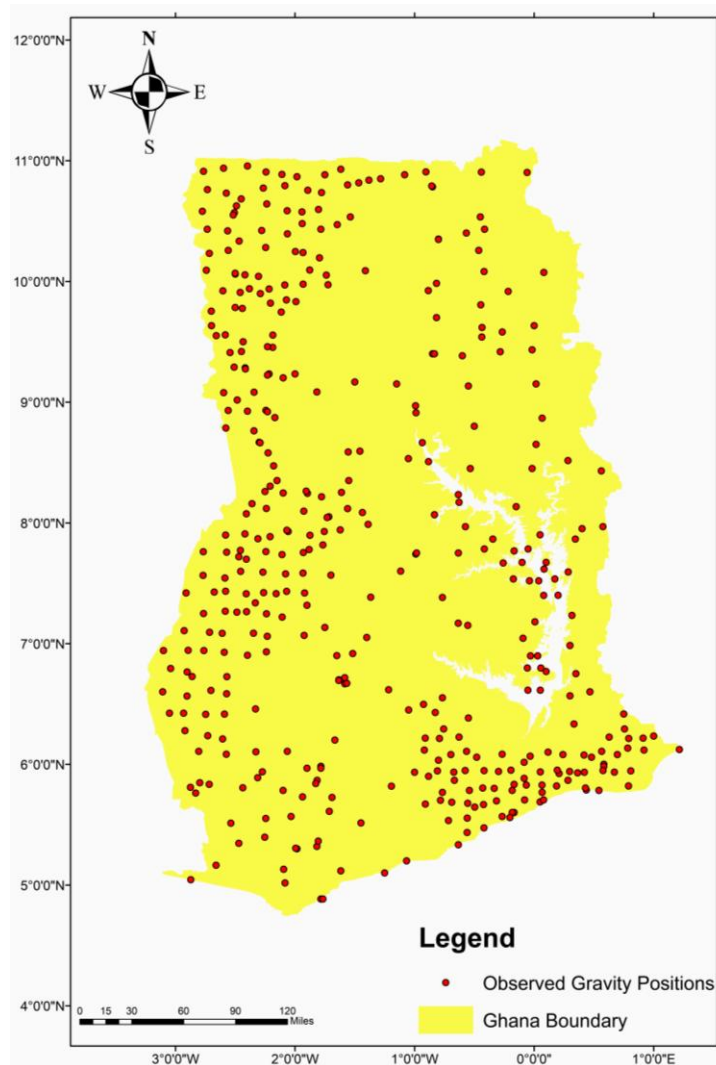


Figure 1. Geospatial Distribution of the Observed Gravity Locations in Ghana

2.2. Overview of Machine Learning Techniques

2.2.1 Backpropagation Neural Network

BPNN is a type of nonlinear and nonparametric technique of ANN (Bishop, 1995). It is developed based on imitating mathematically the functions of the human brain. BPNN consist of densely interconnected nodes called neurons that process information introduced to the network. The general arrangement of the ANN includes the input, hidden and output layers. The function of the input layer is to receive biased weighted signals which are processed and transferred to the hidden layer chamber through an activation function. In the hidden layer, the received signals are encrypted by weights, processed and sent to the output layer. It must be known that the BPNN architecture allows one to increase the hidden layer. However, literature has shown that to solve any real-life problem a single hidden layer is sufficient (Hornik et al., 1989; Park and Sandberg, 1991). The outcomes from the output layer can be expressed in Eq. (1) (Al_Janabi et al., 2018).

$$y_i = f\left(\sum w_{ij}x_i\right) \quad (1)$$

where y_i is the input signal received by a single neuron j . The activation function is defined by f which could be sigmoid or hyperbolic tangent. The existing weights between

neurons i and j and the output from neuron i are shown as w_{ij} and x_i . Turgut (2016) applied BPNN to predict the observed gravity field with satisfactory results. However, in this study, BPNN was used to predict the normal gravity.

2.2.2 Radial Basis Function Neural Network

RBFNN is one of the single layer methods of ANN with a structural design of input, hidden and output layers (Broomhead and Lowe 1988; Sabah et al., 2019). Here, the data collected by the input layer is transferred directly to the hidden layer where the Gaussian activation function is used to transform and handle the nonlinearity in the data. The hidden layer responses are then linearly processed in the output layer to give the predicted outcomes. The network automatically compares the predicted outcomes to the actual to estimate their differences. A decision is then made to minimise the training error function (Eq. (2)) until the desired results are obtained (Al_Janabi et al., 2018).

$$E = \frac{1}{2} \sum_{i=1}^m \sum_{j=1}^n r_j^2(i) \quad (2)$$

where $r_j(i)$ is the error from various output. RBFNN has been proven to show optimum generalisation performance in several geodetic computations (Tierra et al., 2008; Turgut, 2010; Yilmaz and Gullu, 2012). However, it is yet to be used to predict the normal gravity field. Therefore, RBFNN model has been developed in this study to assess its efficiency in predicting the normal gravity.

2.2.3 Group Method of Data Handling

GMDH belongs to the family of polynomial neural networks proposed by Ivakhnenko (1966). The technique is very potent for solving both linear and nonlinear problems related to classification and regression. GMDH technique is made up of several layers of polynomial neurons arranged in a feed-forward manner to determine the mapping relationship between input and output variables. In its modelling procedure, multiple hidden layers are constructed in which the starting layer provides the values for each input predictor variable. The next successive layers constructed then draws its input from the number of neurons in the previous layer. The process continues until the stopping criterion of root mean square error (RMSE) is met. Consequently, the larger the MSE of the proceeding layer than the preceding layer, the GMDH algorithm automatically stops adding layers (Assaleh et al., 2013). Here, the best neuron in the layer that produced the smallest RMSE is selected as the final model output. The GMDH has not been applied to predict normal gravity. Therefore, its suitability as a normal gravity prediction method is investigated in this study. Details of the GMDH mathematical background and theory can be found in (Ivakhnenko, 1966; Ivakhnenko, 1971).

2.2.4 Support Vector Machine

SVM is a machine learning technique developed by Cortes and Vapnik (1995) to solve classification and regression problems. In regression, which is utilised in this study, the technique works by mapping the input information from a low-dimensional feature space and extending it to a higher dimensional solution space using basis function vector. To get very high generalisation performance, the SVM finds the optimal separating hyperplane that maximises the margins of the training data correctly. To do that, the SVM minimise a constraint quadratic programming optimization function (Smola et al., 2004; Ao and Palade, 2011; Xiang-Yang et al., 2011). The SVM regression model (Lessmann, 2012) can be expressed in the form of Eq. (3).

$$y(x) = \sum_{i=1}^N (\beta_i - \beta_i^*) M(x, x_i) + c \quad (3)$$

where β and β^* are the Lagrange multipliers, $M(x, x_i)$ is the kernel function and c is the bias term. In the SVM solution, different kernel functions (such as Gaussian, polynomial, sigmoid and linear (Xuan-Nam, 2019; Güraksin et al., 2014) were tested to select the kernel that adapted efficiently to the training data patterns. Literature has shown that SVM has never been used to predict normal gravity. Hence, its application for this purpose is considered here.

2.2.5 Least Squares Support Vector Machine

The LSSVM is a supervised machine learning method proposed by Suykens et al. (2002) as an extension of SVM for solving function estimation and pattern recognition problems. The LSSVM was used in this study as a function estimation technique to carry out the normal gravity field prediction. The LSSVM solutions are produced by mapping the input data into a higher dimensional space by calibrating well on the training data patterns by finding the best training margin. To achieve the best training margin, the LSSVM minimises the objective function of the optimisation problem by solving a set of linear constraints instead of the quadratic programming found in the SVM (Chugh et al., 2015). The LSSVM regression (Chai, 2015; Hoang, 2014) is given in Eq. (4).

$$y(x) = \sum_{i=1}^N (\alpha_i - \alpha_i^*) K(x_i, x_j) + d \quad (4)$$

where α and α^* are the Lagrange multipliers which can assume positive or negative values due to the linear constraints, $K(x_i, x_j)$ is the kernel function and d is the bias term. In this study, the capability of the LSSVM using radial basis kernel function for predicting normal gravity has for the first time been investigated.

2.2.6 Multivariate Adaptive Regression Splines

MARS approach proposed by Friedman (1991) is a machine learning technique which due to its nonparametric nature can automatically handle nonlinearities and intercommunications among variables. The MARS provides solutions by processing the data at two different stages using the forward selection and backward elimination (Friedman, 1991). Here, several splines are created by splitting the training data on equal interval basis. The training data is split further into different subgroups to create different knots which can be found between the input variables separating the subgroup. The MARS approach creates the regression model by fitting a bended regression line on each of the data found from one subgroup to subgroup and from one spline to another. Here, the basis function defines the approximation with the help of the smoothing splines on each of the subgroup data (Chugh et al., 2015). The MARS model is expressed in Eq. (5).

$$y(x) = b_o + \sum_{i=1}^K BF_i \times c_i \quad (5)$$

where b_o is a constant, BF is the basis function, c_i is the coefficient of the basis function and K is the number of basis function that gave the optimum MARS model. In this study, the strength of MARS approach for predicting normal gravity is investigated.

3. Assessing Model Prediction Accuracy

The Mean Absolute Percentage Error (MAPE), Normalised Root Mean Square Error (NRMSE), Root Mean Square Error (RMSE), Variance Accounted For (VAF) and

Performance Index (PI) served as quality measures to study the robustness of the predictive machine learning models on the data sets used. Here, the predicted values from the developed models were compared with the actual by calculating their respective errors. The mathematical notations for the statistical indicators (Yagiz et al., 2018) used are given in Eqs. (6) to (10).

$$MAPE = \frac{100\%}{N} \sum_{i=1}^N \left| \frac{M_i - P_i}{M_i} \right| \quad (6)$$

$$NRMSE = \frac{RMSE}{M_{\max} - M_{\min}} \quad (8)$$

$$RMSE = \sqrt{\frac{1}{N} \sum_{i=1}^N (M_i - P_i)^2} \quad (7)$$

$$VAF = \left[1 - \frac{\text{var}(M_i - P_i)}{\text{var}(M_i)} \right] \times 100 \quad (9)$$

$$PI = \left[R^2 + \left(\frac{VAF}{100} \right) \right] - NRMSE \quad (10)$$

where M_i is the actual normal gravity computed from Somigliana-Pizetti formula and P_i is the predicted normal gravity field values from the machine learning methods. The M_{\max} and M_{\min} are the maximum and minimum values of the actual normal gravity. N denotes the total observation points and i takes values from 1 to N .

4. Developed Machine Learning Normal Gravity Predictive Models

To develop the normal gravity prediction models using the six machine learning methods, the 424 observation data was partitioned into two sets, namely training and testing. The training set was used to train and fit the model to adapt to the data set while the testing data was used as unseen data for which predictions must be made to validate the selected optimum trained model. Literature reviewed (Shahin, 2000 and references therein) indicates that the selected training and testing data points for machine learning modelling must have very closely related statistical properties that represent the same population. This rule of thumb is necessary because if the range of testing data is completely outside the training data range, there is the likelihood to experience overfitting. In such cases, the model predictions for the test data poorly match those obtained using the training data. Therefore, judging the validity of the machine learning models becomes a challenge (Maier and Dandy, 2000). This is consistent with Tokar and Johnson (1999) research findings which indicate that the manner in which the data set is divided do have influence on the final outputs.

However, to overcome these limitations, scholars (Masters, 1993; Shahin, 2000 and references therein) have proposed that statistical properties such as mean, minimum, maximum, standard deviation and range of the training and testing datasets must belong to the same sample population. Consequently, Table 2 presents the statistical properties of the data set (training and testing) used. From Table 2, it can be noticed that the reported values for training and testing data can be found within the same range and thus satisfy the data division criteria as stipulated in the literature.

Table 2. Statistical Properties of the Selected Training and Testing Data Points

Statistical Parameters	Training (mGal)	Testing (mGal)
Minimum	978070.0932	978073.9583
Maximum	978219.1795	978217.5069
Range	149.086355	143.548579
Mean	978130.873	978130.7025
Standard Deviation	43.734	42.375

Furthermore, visual observation of Figure 2 shows that the purposefully selected training data covers the entire study area which provides a better characteristic representation of the data. Similarly, the testing data are evenly spread out across the study area (Figure 2). As a result, 297 of the 424 total data points were used to train the models (approximately 70%), and the remaining 127 data points (approximately 30%) were used for model performance evaluation. In the modelling, latitude, longitude and elevation served as the input parameters, while, the output parameter was the normal gravity. In order to fulfill the supervised machine learning condition, the normal gravity was first calculated using the Somigliana-Pizzetti formula (Eq. (11)). The choice of using Eq. (11) among other equations is because of its rigorous ability to globally estimate the normal gravity with minimal uncertainties as reported in previous studies (Vajda and Pánisová, 2005; Okiwelu et al., 2010). The simplicity of Eq. (11) is well noted. However, as indicate earlier, the knowledge on how the machine learning approach can handle this topic has some scientific value worth investigating. Ultimately, as the world embraces artificial intelligence as a revolutionised technology, a study on the predictive strengths and feasibility of machine learning in handling normal gravity is significant.

$$\gamma = 978032.53349 \left[\frac{1 + 0.00193185265241 \sin^2 \varphi}{\sqrt{1 - 0.00669437999013 \sin^2 \varphi}} \right] \text{mgal} \quad (11)$$

where φ is the geodetic latitude.

Because the data was obtained and compiled from different sources, there is high existence of data variability. Therefore, as a first step in developing the machine learning models, the data set was normalised into the range [-1, 1] using Eq. (12) (Muller and Hemond, 2013).

$$g_i = g_{\min} + \frac{(g_{\max} - g_{\min}) \times (u_i - u_{\min})}{(u_{\max} - u_{\min})} \quad (12)$$

where g_i represents the normalised data, u_i is the actual normal gravity values obtained from the Somigliana-Pizzetti formula, while u_{\min} and u_{\max} represent the minimum and maximum value of the actual normal gravity with g_{\max} and g_{\min} values set at 1 and -1.

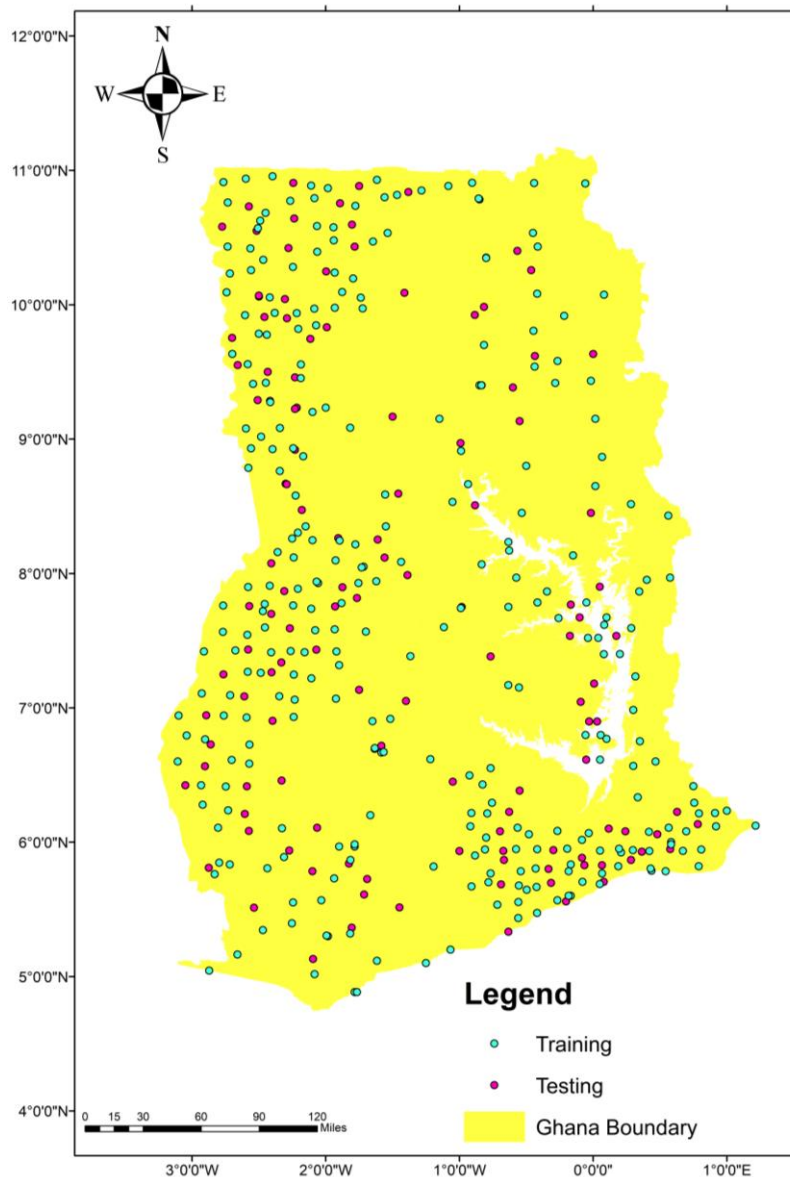


Figure 2. Training and Testing Data Distributions in Ghana

4.1 BPNN Model

Selecting the optimum BPNN model is deeply dependent on the hidden layer and hidden nodes that will produce the least RMSE value. One hidden layer which is enough to universally approximate any data set (Hornik et al., 1989; Park and Sandberg, 1991) was adopted in the model development. To find the optimal hidden nodes, the widely used progressive trial and error approach (Nguyen et al., 2019) was adopted. In the training stage, the hidden nodes was set to the interval [1-20]. This limit was set because the RMSE got worse when the hidden nodes went beyond 20. The Bayesian regularisation backpropagation (Buntine and Weigend, 1991) was used as the training algorithm. The hyperbolic tangent and linear activation functions (Mathias and Rech, 2012) were used in the hidden and output layers, respectively. The BPNN structure that produced the best performance was [3-20-1]. That is three inputs, twenty hidden nodes and one output.

4.2 RBFNN Model

In RBFNN, only the width parameter (σ) and maximum number of neurons are mostly adjusted to monitor the model’s performance. The σ values were set in the range of 1 to 13 during the training phase. It was observed that values beyond 13 was not given any meaningful results. After monitoring several training trials, the optimum RBFNN structure that produced the best performance based on RMSE was [3-50-1], thus three inputs, 50 neurons and one output having σ value of 13.

4.3 GMDH Model

Contrary to other ANN methods, the GMDH-type ANN is a multi-layered system which is broadly defined by a compact set of polynomials and does not require its architecture to be predetermined. The evolutionary principle mostly used as the GMDH training algorithm (Ivakhnenko, 1966; Ivakhnenko, 1971; Assaleh et al., 2013) is adopted in this study. For quality control, a penalty term based on the RMSE criterion is used to avoid overtraining. Thus, model complexity is controlled automatically by the GMDH using the penalty term. Here, the training process is stopped when a minimum RMSE value is achieved. With this, the GMDH model predictive capability is known. It is important to note that the different layers, neurons and models formed at each training stage are automatically determined because of the GMDH self organising system. The technique also has feature extraction ability to select the most highly significant input variables in predicting the output. Table 3 shows the number of layers, neurons for each successive layers formed and their corresponding equations. It can be seen that out of the three input variables (latitude, longitude, height), the GMDH selected only the latitude and longitude as the most significant parameters in the modelling processes.

Table 3. GMDH Model Network Architecture and Equations

Layer No.	No. of Neurons	Equation
1	1	$x_4 = 978030.869113 - 0.0129283648607(\lambda) + 0.638423719102(\varphi) + 0.000603118118346(\lambda \times \varphi) - 0.00283028743667(\varphi)^2 + 1.51108789836(\lambda)^2$
2	1	$x_7 = 511389.039208 - 0.0375309382884(x_4) + 3034.68130755(\varphi) - 0.00310373826721(\varphi \times x_4) + 5.26217565922e - 07(x_4) + 0.126820624351(\varphi)^2$
3	1	$x_{10} = 371696.289774 + 0.240006605526(x_7) + 22.8503318125(\lambda) - 2.33531197681e - 05(\lambda \times x_7) + 3.88482463476e - 07(x_7)^2 + 0.00272037510912(\lambda)^2$
4	1	$x_{13} = 392909.090825 - 0.273976745627(x_{10}) - 1286.7031043(\varphi) + 0.00131569598307(\varphi \times x_{10}) + 8.91833684042e - 07(x_{10})^2 - 0.760921698698(\varphi)^2$

5	1	$x_{16} = -374456.232067 + 0.506375465584(x_{13}) - 3930.15107499(\varphi)$ $+ 0.00401878514267(\varphi \times x_{13}) + 8.96177297082e - 07(x_{13})$ $- 2.05257649354(\varphi)^2$
6 (Final Model)	1	$\text{Normal Gravity} = 345378.109135 + 0.23274003374(x_{16}) - 122.516823945(\varphi)$ $+ 0.000125269594529(\varphi \times x_{16}) + 4.23425958174e - 07(x_{16})^2$ $- 0.0971940002278(\varphi)^2$

4.4 SVM Model

In the SVM modelling, different kernel functions such as linear, polynomial and Gaussian were tested. The polynomial kernel function of order two outperformed all the other tested kernels and was therefore applied to develop the SVM normal gravity field prediction model. In addition, the optimum hyper-parameters (ε and C) that regulates the performance of the SVM model was determined using sequential trial and error procedure (Tseng et al., 2016). Consequently, the optimum SVM model that produced the least RMSE in both training and testing had $\varepsilon = 0.00000001$ and $C = 50$, respectively.

4.5 LSSVM Model

With the LSSVM, two hyper-parameters including the regularization parameter (γ) and the width of the radial basis kernel function (σ) were fine tuned to get the optimal prediction results. The simplex search algorithm (De Brabanter et al., 2010) was applied to determine the optimal values for γ and σ . As a results, optimum designed values for γ and σ were 26850520130.0918 and 83.8691537704513, respectively.

4.6 MARS Model

Among the different piecewise order of interactions, the zero order produced the optimal MARS model by achieving the least RMSE value. In the modelling, the maximum selected number of basis functions used for the forward phase were 30 out of which 14 were eliminated as redundant in the backward elimination process. At the end, the final model (Eq. (13)) had 16 selected basis functions with their corresponding equations as shown in Table 4. It can be seen from the table that only one out of the three input parameters was selected to form the final model. Thus, the latitude was selected leaving out longitude and height (see Table 4). This situation is usually encountered when using the MARS approach because of its pruning and feature extraction ability to select the most significant predictor variable and basis functions to create the model. This then leads to formulating simple and less complicated explanatory model. The procedural dynamics of the MARS model has already been given in Friedman (1991) when the author first introduced the method.

$$\text{Normal Gravity MARS Model} = 978123 + \sum_{i=1}^{16} BF_i \times b_i \tag{13}$$

where BF_i is the basis function and b_i is the coefficient of the basis function.

Table 4. List of Basis Functions (BF_i) of the Optimum MARS Model and their Corresponding Equations

BF_i	Equations	b_i
BF ₁	$\max(0, \varphi - 8.085)$	17.2726
BF ₂	$\max(0, 8.085 - \varphi)$	-16.4633
BF ₃	$\max(0, \varphi - 6.23333)$	1.369
BF ₅	$\max(0, \varphi - 9.63267)$	1.49707
BF ₇	$\max(0, \varphi - 7.16833)$	0.891953
BF ₉	$\max(0, \varphi - 8.785)$	1.23749
BF ₁₁	$\max(0, \varphi - 5.56667)$	1.59145
BF ₁₃	$\max(0, \varphi - 10.28)$	1.39694
BF ₁₅	$\max(0, \varphi - 7.73667)$	1.11091
BF ₁₇	$\max(0, \varphi - 6.765)$	1.59136
BF ₁₉	$\max(0, \varphi - 5.9)$	0.803778
BF ₂₁	$\max(0, \varphi - 9.15)$	1.18816
BF ₂₃	$\max(0, \varphi - 8.35)$	1.10099
BF ₂₅	$\max(0, \varphi - 10.7728)$	1.26258
BF ₂₇	$\max(0, \varphi - 7.41833)$	0.79737
BF ₂₉	$\max(0, \varphi - 9.97167)$	0.56414

5. Results and Discussion

The practical performance assessment of any developed model lies in its ability to predict the testing data set appropriately. This is because the testing data is used to independently assess the model adequacy since it does not contribute to the initial model development process. Consequently, a good model is accepted as excellent predictor when it can generalise well on the unseen data set (testing). Table 5 shows the results for both training and testing data respectively. Looking at the table, it is observed that no overfitting situation was experienced as the models could calibrate and generalise correctly on both training and testing data. Several performance criteria presented in Table 5, Figures 3 and 4 were used to evaluate the various models performance. To be able to apply the performance metrics (Eqs. (6) to (10)), the error difference between the actual and predicted normal gravity values obtained from each method were used. Ideally, when a predictive model RMSE is equal to zero then that model is accepted and claimed to be excellent. In Table 5, it can be seen that RBFNN, BPNN, LSSVM, GMDH, SVM and MARS had both training and testing RMSE values approaching zero. This means that the predictions produced by these models deviated slightly from the actual normal gravity values. Furthermore, the NRMSE expressed as a percentage is also a goodness of fit indicator to check the performance of each model.

Theoretically, a model with lower NRMSE values indicate less residual variance. That is, the lower the NRMSE value the better model performance. Therefore, a careful study of Table 5 shows that the RBFNN, BPNN, LSSVM, GMDH, SVM and MARS had fewer residual variations for the training and testing data. From the NRMSE results (Table 5), it can be stated that the unexplained variability in the predicted normal gravity when compared with the actual was very small. The MAPE further confirms the strength of the developed RBFNN, BPNN, LSSVM, GMDH, SVM and MARS models, respectively.

Table 5. Performance of the Different Machine Learning Models

Training			
Model	RMSE (mGal)	NRMSE (%)	MAPE (%)
RBFNN	2.81E-05	1.89E-05	2.05E-09
BPNN	6.04E-05	4.05E-05	5.00E-09
LSSVM	1.13E-04	7.60E-05	8.24E-09
GMDH	1.04E-03	7.00E-04	8.85E-08
SVM	3.95E-02	2.65E-02	3.66E-06
MARS	4.23E-02	2.84E-02	3.53E-06
Testing			
RBFNN	2.93E-05	5.97E-10	2.20E-09
BPNN	5.67E-05	2.24E-09	4.90E-09
LSSVM	1.35E-04	1.26E-08	9.59E-09
GMDH	9.32E-04	6.05E-07	8.10E-08
SVM	4.04E-02	1.14E-03	3.72E-06
MARS	4.15E-02	1.20E-03	3.50E-06

For each model, the computed VAF (Eq. (9)) and PI (Eq. (10)) values for the testing data are presented graphically in Figures 3 and 4, respectively. The VAF indicate the correctness of a model by comparing the models output to the actual data. Therefore, the higher the VAF values the better the model’s predictive strength. In Figure 3, it can be seen that almost all the models obtained a VAF value above 99% which indicate that the developed models are efficient to be used to predict the normal gravity. To further examine the accuracy of the models developed, PI statistic was used. Judging from Figure 4, it is observed that all the models had PI values approaching two. This means that the predictions produced by RBFNN, BPNN, LSSVM, GMDH, SVM and MARS are highly precise. Although all the machine learning models performed creditably well, it is recognisable from the results (Table 5, and Figures 3 and 4) that the RBFNN seems to be the most robust and efficient accurate predictor of the normal gravity than the other methods investigated. This model predictive efficiency was closely followed by BPNN, GMDH, LSSVM, SVM and MARS in that order.

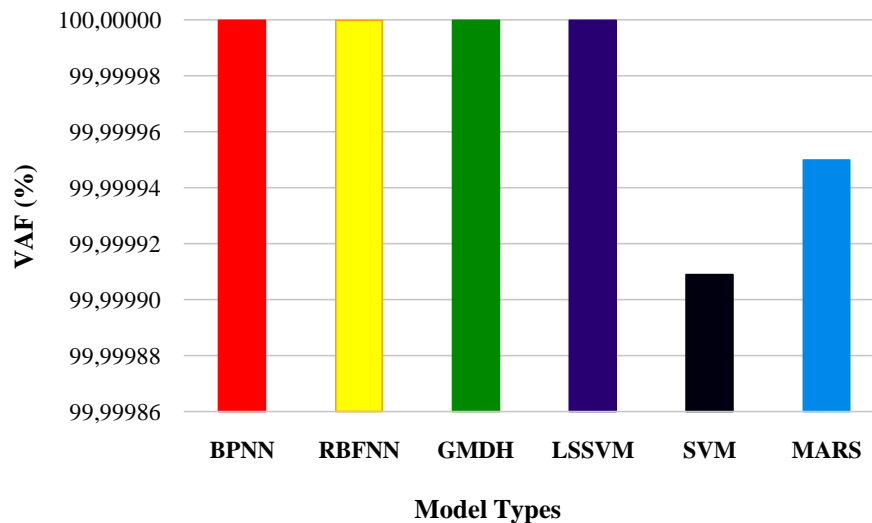


Figure 3. Computed VAF for each Model Based on Test Data

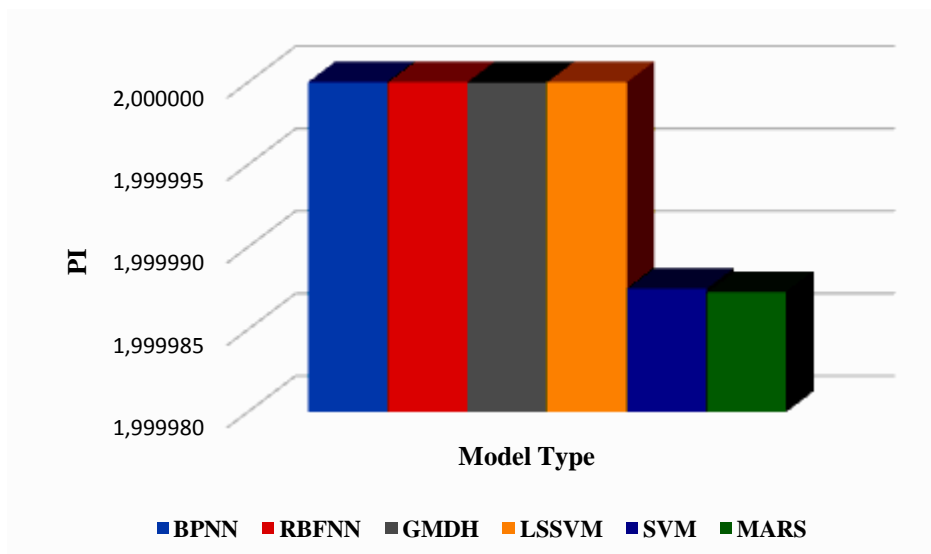


Figure 4. Computed PI Statistic for each Model Based on the Test Data

Practically, the reported predictions based on their respective statistical evaluators (RMSE, NRMSE, MAPE, VAF and PI) indicated that the tested machine learning techniques (RBFNN, BPNN, LSSVM, GMDH, SVM and MARS) have adequately modelled the normal gravity. Therefore, applying the supervised learning approach is a suitability to model and predict the normal gravity.

6. Conclusions

The current dispensation of moving into a digital world in the fourth industrial revolution has machine learning central to its success. Therefore, a study to assess the capability of machine learning in normal gravity prediction has some scientific value worth investigating. In this paper, six widely used machine learning models in literature including RBFNN, BPNN, LSSVM, GMDH, SVM and MARS have been tested in predicting normal gravity. A total of 424 historical observed gravity location data from Bureau Gravimétrique

International (BGI) and Ziwu (2011) acquired from the Ghana Geological Survey Authority was used to establish the prediction models. The supervised learning approach was adopted in the model building. The predictive capabilities of the models were evaluated using MAPE, RMSE, NRMSE, VAF and PI. Overall, the predictions from RBFNN, BPNN, LSSVM, GMDH, SVM and MARS agreed very well with the actual normal gravity values. Comparatively, the RBFNN was the most robust and efficient technique. In conclusion, it was found that the machine learning models proposed in this study are reliable and acceptable advance computational tools for the normal gravity prediction and have the ability to generalise appropriately.

7. References

1. Abbak, R.A., Ustun, A., 2015: *A software package for computing a regional gravimetric geoid model by the KTH method*. *Earth Science Informatics*, 8, 1, 255-265.
2. Al_Janabi, S., Al_Shourbaji, I., Salman, M.A., 2018: *Assessing the suitability of soft computing approaches for forest fires prediction*. *Applied Computing and Informatics*, 14, 2, 214-224.
3. Anyah, R.O., Forootan, E., Awange, J.L., Khaki, M., 2018: *Understanding linkages between global climate indices and terrestrial water storage changes over Africa using GRACE products*. *Science of the Total Environment*, 635, 1405-1416.
4. Ao, S. I., Palade, V., 2011: *Ensemble of Elman neural networks and support vector machines for reverse engineering of gene regulatory networks*. *Applied Soft Computing*, 11, 1718-1726. <https://doi.org/10.1016/j.asoc.2010.05.014>
5. Ardalan, A.A., Grafarend, E.W., 2001: *Somigliana–Pizzetti gravity: the international gravity formula accurate to the sub-nanoGal level*. *Journal of Geodesy*, 75, 7-8, 424-437.
6. Assaleh, K., Shanableh, T., Kheil, Y.A., 2013: *Group method of data handling for modeling magnetorheological dampers*. *Intelligent Control and Automation*, 4, 1, 70-79.
7. Awange, J., Kiema, J.B., 2013: *Environmental Geoinformatics. Second Edition*, Berlin, Heidelberg: Springer Berlin Heidelberg, 10, 978-3, <https://doi.org/10.1007/978-3-030-03017-9>.
8. Bishop, C. M., 1995: *Neural networks for pattern recognition*. UK: Oxford Press.
9. Broomhead, D.S., Lowe, D., 1988: *Multivariable functional interpolation and adaptive networks*. *Complex Systems*, 2, 321-355.
10. Buntine, W.L., Weigend, A.S., 1991: *Bayesian backpropagation*. *Complex systems*, 5, 6, 603-643.
11. Bureau Gravimetricque International (BGI). DOI:10.18168/BGI
12. Cao, Y., Nan, Z., Cheng, G., 2015: *GRACE gravity satellite observations of terrestrial water storage changes for drought characterization in the arid land of northwestern China*. *Remote Sensing*, 7, 1, 1021-1047.
13. Chai, J., Du, J., Lai, K.K., Lee, Y.P., 2015: *A hybrid least square support vector machine model with parameters optimization for stock forecasting*. *Mathematical Problems in Engineering*, Volume 2015, Article ID 231394, 1-7.
14. <http://dx.doi.org/10.1155/2015/231394>
15. Chugh, M., Thumsi, S., Keshri, V., 2015: *A comparative study between least square support vector machine (LS-SVM) and multivariate adaptive regression spline (MARS) methods for the measurement of load storing capacity of driven piles in cohesive less soil*. *International Journal of Structural and Civil Engineering Research*, 4, 2, 189-194.

16. Cortes, C., Vapnik, V., 1995: *Support-Vector Networks*. *Machine Learning*, 20, 3, 273-297.
17. Dabove, P., Manzano, A.M., 2017: *Artificial neural network for detecting incorrectly fixed phase ambiguities for L1 mass-market receivers*. *GPS Solutions*, 21, 3, 1213-1219.
18. De Brabanter, K., Karsmakers, P., Ojeda, F., Alzate, C., De Brabanter, J., Pelckmans, K., De Moor, B., Vandewalle, J., Suykens, J.A., 2010: *LS-SVMLab toolbox user's guide: version 1.8*, Katholieke Universiteit Leuven.
19. Forootan, E., Khaki, M., Schumacher, M., Wulfmeyer, V., Mehrnegar, N., van Dijk, A.I.J.M., Brocca, L., Farzaneh, S., Akinluyi, F., Ramillien, G., Shum, C.K., 2019: *Understanding the global hydrological droughts of 2003–2016 and their relationships with teleconnections*. *Science of the Total Environment*, 650, 2587-2604.
20. Friedman, J.H., 1991: *Multivariate Adaptive Regression Splines*. *The Annals of Statistics*, 19, 1, 1-141.
21. González M.F., Nunes, J.C., Arnosó, J., Luque Martínez, T., Medeiros, S., Benavent, M., Vieira, R., 2010: *Inferences from gravity data interpretation of the volcanic complexes of the Terceira Island (Azores)*. *Geophysical Research Abstracts*, 12, EGU2010-4435-1, 1.
22. Gullu, M., Narin, O.G., 2019: *Georeferencing of the Nile River in Piri Reis 1521 map, Using Artificial Neural Network Method*. *Acta Geodaetica et Geophysica*, 1-15. <https://doi.org/10.1007/s40328-019-00255-7>
23. Güraksin, G. E., Hakli, H., Harun, U., 2014: *Support vector machines classification based on particle swarm optimization for bone age determination*. *Applied Soft Computing*, 24, 597-602. <https://doi.org/10.1016/j.asoc.2014.08.007>
24. Hans-Jürgen, G., 2011: *International Gravity Formula*. Found in *Solid EARTH Geophysics*,
25. Hassan, A. and Jin, S., 2016: *Water storage changes and balances in Africa observed by GRACE and hydrologic models*. *Geodesy and Geodynamics*, 7, 1, 39-49.
26. Heiskanen, W. A., Moritz, H., 1967: *Physical Geodesy*. San Francisco: W. H. Freeman.
27. Hoang, N.D., Pham, A.D., Cao, M.T., 2014: *A novel time series prediction approach based on a hybridization of least squares support vector regression and swarm intelligence*. *Applied Computational Intelligence and Soft Computing*, Volume 2014, Article ID 754809, 1-8.
28. <http://dx.doi.org/10.1155/2014/754809>
29. Hornik, K., Stinchcombe, M., White, H., 1989: *Multilayer feed forward networks are universal approximators*. *Neural Networks*, 2, 359-366.
30. Huang, F.M., Wu, P., Ziggah, Y.Y., 2016: *GPS monitoring landslide deformation signal processing using time-series model*. *International Journal of Signal Processing, Image Processing and Pattern Recognition*, 9, 3, 321-332.
31. Isioye, O.A., 2010: *Normal Gravity and the Nigerian Height System*. *FS 1C - Geoid and Gravity - Modelling, Measurements and Applications*. *FIG Congress 2010 Facing the Challenges-Building the Capacity Sydney, Australia, 11-16 April 2010*, 1-13.
32. Ivakhnenko, A. G., 1966: *Group method of data handling a rival of the method of stochastic approximation*. *Soviet Automatic Control*, 13, 43-71.
33. Ivakhnenko, A. G., 1971: *Polynomial Theory of Complex Systems*. *IEEE Transactions on Systems, Man and Cybernetics*, 4, 364-378.
34. Jacoby, W., Smilde, P.L., 2009: *Gravity interpretation: fundamentals and application of gravity inversion and geological interpretation*. Springer Science & Business Media.

35. Kaftan, I., Salk, M., Senol, Y., 2011: *Evaluation of gravity data by using artificial neural networks case study: Seferihisar geothermal area (Western Turkey)*. *Journal of Applied Geophysics*, 75, 4, 711-718.
36. Kenfack, J.V., Tadjou, J.M., Kamguia, J., Tabod, T.C., Bekoa, A., 2011: *Gravity Interpretation of the Cameroon Mountain (West Central Africa) Based on the New and Existing Data*. *International Journal of Geosciences*, 2, 04, 513-522.
37. Kingdon, R., 2012: *Advances in gravity based height systems*. PhD Dissertation, University of New Brunswick, Canada.
38. Kusche, J., Springer, A., 2017: *Parameter estimation for satellite gravity field modeling*. In *Global Gravity Field Modeling from Satellite-to-Satellite Tracking Data*, 1-34, Springer, Cham, Switzerland.
39. Lakshmanan, J., 1991: *The generalized gravity anomaly: endoscopic microgravity*. *Geophysics*, 56, 712–723.
40. Leaman, D.E., Webster, S.S., 2002: *Quantitative interpretation of magnetic and gravity data for the Western Tasmanian Regional Minerals Program*. *Tasmanian Geological Survey Record 2002/15*, Mineral Resources Tasmania, Department of Infrastructure and Energy resources, 1-8.
41. Lei, Y., Zhao, D., Cai, H., 2015: *Prediction of length-of-day using extreme learning machine*. *Geodesy and Geodynamics*, 6, 2, 151-159.
42. Lessman, S., Sung, M.C., Johnson, J.E., 2012: *Adapting least-square support vector regression models to forecast the outcome of horseraces*. *The Journal of Prediction Markets*, 1, 3, 169-187.
43. Li, X., Götze, H.-J., 1996: *Effects of topography and geoid on gravity anomalies in mountainous areas: the central Andes as an example*. *Institut für Geologie, Geophysik und Geoinformatik, Freie Universität Berlin*.
44. Li, X., Götze, H.-J., 2001: *Ellipsoid, geoid, gravity, geodesy and geophysics*. *Geophysics*, 66, 1660–1668.
45. Li, X., Götze, H.-J., 2001: *Ellipsoid, geoid, gravity, geodesy and geophysics*. *Geophysics*, 66, 1660-1668.
46. Liao, D.C., Wang, Q.J., Zhou, Y.H., Liao, X.H., Huang, C.L., 2012: *Long-term prediction of the earth orientation parameters by the artificial neural network technique*. *Journal of Geodynamics*, 62, 87-92.
47. Maier, H. R., Dandy, G.C., 2000: *Neural networks for the prediction and forecasting of water resources variables: a review of modelling issues and applications*. *Environmental Modelling and Software*, 15, 101-124.
48. Masters, T., 1993: *Practical neural network recipes in C++*, Academic Press, Inc., San Diego, California.
49. Mathias, A.C., Rech, P.C., 2012: *Hopfield neural network: the hyperbolic tangent and the piecewise-linear activation functions*. *Neural Networks*, 34, 42-45.
50. Moritz, H., 1980: *Geodetic reference system*. *Bulletin Géodésique*, 54, 395–405.
51. Mugnier, J. C., 2000: *OGP-Coordinate conversions and Transformations including formulae*. *COLUMN, Grids and Datums, The Republic of Ghana*. *Photogrammetric Engineering and Remote Sensing*, 695-697.
52. Muller, V.A., Hemond, F.H., 2013: *Extended artificial neural networks: incorporation of a priori chemical knowledge enables use of ion selective electrodes for in-situ measurement of ions at environmentally relevant levels*. *Talanta*, 117, 112–118.

53. Nguyen, H., Drebenstedt, C., Bui, X.N., Bui, D.T., 2019: Prediction of Blast-Induced Ground Vibration in an Open-Pit Mine by a Novel Hybrid Model Based on Clustering and Artificial Neural Network. *Natural Resources Research*, 1-19.
54. Okiwelu, A.A., Okwueze, E.E., Onwukwe, C.E., 2010: Evaluation of Accuracy of the Geodetic Reference Systems for the Modelling of Normal Gravity Fields of Nigeria. *Applied Physics Research*, 2, 2, 25-40.
55. Okwuashi, O., Ndehedehe, C., 2015: Digital terrain model height estimation using support vector machine regression. *South African Journal of Science*, 111, 9-10, 01-05.
56. Osazuwa, I. B., 1993: An evaluation study of the correct computational approach for the conversion of gravimetric data from one reference datum to another. *Survey review*, 32, 249, 167-174.
57. Park, J., Sandberg, I.W., 1991: Universal approximation using radial basis function networks. *Neural Computation*, 3, 2, 246-257.
58. Razin, M.R.G., Voosoghi, B., 2017: Ionosphere tomography using wavelet neural network and particle swarm optimization training algorithm in Iranian case study. *GPS Solutions*, 21, 3, 1301-1314.
59. Rybakov, M., Goldshmidt, V., Fleischer, L., Ben-Gai, Y., 2000: 3-D gravity and magnetic interpretation for the Haifa Bay area (Israel). *Journal of Applied Geophysics*, 44, 4, 353-367.
60. Sabah, M., Talebkeikhah, M., Wood, D.A., Khosravanian, R., Anemangely, M., Younesi, A., 2019: A machine learning approach to predict drilling rate using petrophysical and mud logging data. *Earth Science Informatics*, pp.1-21. <https://doi.org/10.1007/s12145-019-00381-4>
61. Salim, A.M., Dwarakish, G.S., Liju, K.V., Thomas, J., Devi, G., Rajeesh, R., 2015: Weekly prediction of tides using neural networks. *Procedia Engineering*, 116, 678-682.
62. Sedlak, J., Gnojek, I., Zabadal, S., Farbisz, J., Cwojdzinski, S., Scheibe, R., 2007: Geological interpretation of a gravity low in the central part of the Lugian Unit (Czech Republic, Germany and Poland). *Journal of Geosciences*, 52, 3-4, 181-197.
63. Shahin, M.A., Maier, H.R., Jaksa, M.B., 2000: Evolutionary data division methods for developing artificial neural network models in geotechnical engineering. *Research Report No. R 171, University of Adelaide, Department of Civil and Environmental Engineering*.
64. Smola, A., Schölkopf, B., 2004: A tutorial on support vector regression. *Statistics and Computing*, 14, 199-222. <https://doi.org/10.1023/B:STCO.0000035301.49549.88>
65. Suykens, J. A. K., Van Gestel, T., De Brabanter, J., De Moor, B., & Vandewalle, J. (2002). *Least squares support vector machines*. World Scientific, Singapore.
66. Tierra, A., Dalazoana, R., De Freitas, S., 2008: Using an artificial neural network to improve the transformation of coordinates between classical geodetic reference frames. *Computers & Geosciences*, 34, 181-189. <https://doi.org/10.1016/j.cageo.2007.03.011>
67. Tierra, A.R., De Freitas, S.R.C., 2005: Artificial neural network: a powerful tool for predicting gravity anomaly from sparse data. In *Gravity, Geoid and Space Missions*, Springer, Berlin, Heidelberg, 208-213.
68. Tokar, A.S., Johnson, P.A., 1999: Rainfall-runoff modeling using artificial neural networks. *Journal of Hydrologic Engineering*, 4, 3, 232-239.
69. Tseng, T.L.B., Aleti, K.R., Hu, Z., Kwon, Y.J., 2016: E-quality control: A support vector machines approach. *Journal of Computational Design and Engineering*, 3, 2, 91-101.
70. Turgut, B., 2010: A back-propagation artificial neural network approach for three-dimensional coordinate transformation. *Scientific Research Essays*, 5, 21, 3330–3335.

71. Turgut, B., 2016: *Application of back propagation artificial neural networks for gravity field modelling. Acta Montanistica Slovaca*, 21, 3, 200-207.
72. Vajda, P., Pánisová, J., 2005: *Practical comparison of formulae for computing normal gravity at the observation point with emphasis on the territory of Slovakia. Contributions to Geophysics and Geodesy*, 35, 173-188.
73. Vanicek, P., Krakiwsky, E.J., 1986: *Geodesy: The concept*, Elsevier Science, 2nd Edition, pp.70-96.
74. Wang, H., Xiang, L., Jia, L., Wu, P., Steffen, H., Jiang, L., Shen, Q., 2015: *Water storage changes in North America retrieved from GRACE gravity and GPS data. Geodesy and Geodynamics*, 6, 4, 267-273.
75. Wang, W., Yuan, H., 2018: *A Tidal Level Prediction Approach Based on BP Neural Network and Cubic B-Spline Curve with Knot Insertion Algorithm. Mathematical Problems in Engineering*, Volume 2018, Article ID 9835079, 1-9.
76. <https://doi.org/10.1155/2018/9835079>
77. Xiang-Yang, W., Jing-Wei, C., Hong-Ying, Y., 2011: *A New integrated SVM classifiers for relevance feedback content-based image retrieval using EM parameter estimation. Applied Soft Computing*, 11, 2, 2787-2804.
78. Xuan-Nam, B., Nguyen, H., Hai-An, L., Hoang-Bac, B., Ngoc-Hoan, D., 2019: *Prediction of blast-induced air over-pressure in open-pit mine: assessment of different artificial intelligence techniques. Natural Resources Research*, 1-21.
79. Yagiz, S., Ghasemi, E., Adoko, A.C., 2018: *Prediction of rock brittleness using genetic algorithm and particle swarm optimization techniques. Geotechnical and Geological Engineering*, 36, 6, 3767-3777.
80. Yilmaz, I., Gullu, M., 2012: *Georeferencing of historical maps using back propagation artificial neural network. Experimental Techniques*, 36, 5, 15-19.
81. Yilmaz, N., 2008: *Comparison of different height systems. Geo-spatial Information Science*, 11, 3, 209-214.
82. Ziggah, Y.Y., Hu, Y., Issaka, Y., Laari, P.B., 2019: *Least squares support vector machine model for coordinate transformation. Geodesy and Cartography*, 45, 1, 16-27.
83. Ziwu, F.D., 2011: *Determination of the free-air gravity anomalies over Brong-Ahafo region of Ghana. Master Thesis, Kwame Nkrumah University of Science and Technology.*